Pinipay *et al. Clinical Phytoscience* (2023) 9:7
https://doi.org/10.1186/s40816-023-00359-2

Clinical Phytoscience

ORIGINAL CONTRIBUTION

Open Access

Evaluating the anti-urolithiasis potential of *Ficus religiosa* seed GC MS evaluated phytoconstituents based on their in-vitro antioxidant properties and in-silico ADMET and molecular docking studies

Felicity Pinipay[1*], Rajesh Rokkam[1], Satyanarayana Botcha[1] and Raghava Rao Tamanam[1]

Abstract

Background Urolithiasis, the deposit of stones in the urinary tract is a pertinent clinical issue in daily practice that imposes a burden on the human health system. *Ficus religiosa* plant has historically been useful in preventing urolithiasis. There is currently no information on phytochemical profiling that specifies the precise phytochemicals in the seed that are active against urolithiasis.

Methods *F. religiosa* seeds were extracted with different solvents in increasing order of their polarity by Soxhlet extraction. All the extracts were evaluated for their antioxidant potential. GC–MS profiling of the most potent antioxidant *F. religiosa* seed extract was done to evaluate the phytoconstituents. To evaluate the pharmacokinetics and drug-likeness properties of these compounds in silico ADMET analysis was done. To comprehend the binding potential of the best ADMET evaluated phytochemicals contained in the *F. religiosa* seed extract against the several protein targets (matrix metalloproteinases (MMP-2, MMP-9), and Human calcium-sensing receptor (CaSR)) and antioxidant enzymes (Glutathione S-transferase (GST), glutathione-disulfide reductase (GR), glutathione peroxidase (GPX), and superoxide dismutase (SOD)) involved in urolithiasis, multi targets based virtual screening tests were done using Autodock Vina tool.

Results GC–MS profiling revealed the presence of 53 different compounds. Of all these compounds, based on ADMET analysis 2-Methoxy-4-vinylphenol; 3,5-Di-tert-butylphenol; diethyl benzene-1,2-dicarboxylate; 4-hydroxy-3,5-dimethoxybenzaldehyde; 2-methoxy-4-prop-2-enylphenol; and bis (2-methyl propyl) benzene-1,2-dicarboxylate were found to have best pharmacokinetics and drug-likeness properties. In the autodocking studies, 3,5-Di-tert-butyl phenol is proved to be the best of all in terms of binding energies with the selected targets.

Conclusion The findings of this study suggest a framework for employing *F. religiosa* seed ethyl acetate extract as a potent herbal treatment for urolithiasis.

Keywords Urolithiasis, Antioxidant, GC–MS profiling, ADMET, Autodock

*Correspondence:
Felicity Pinipay
felicityosteen@gmail.com
[1] Department of Biochemistry, College of Science and Technology, Andhra University, South Campus, Visakhapatnam 530003, Andhra Pradesh, India

Springer Open

© The Author(s) 2023. **Open Access** This article is licensed under a Creative Commons Attribution 4.0 International License, which permits use, sharing, adaptation, distribution and reproduction in any medium or format, as long as you give appropriate credit to the original author(s) and the source, provide a link to the Creative Commons licence, and indicate if changes were made. The images or other third party material in this article are included in the article's Creative Commons licence, unless indicated otherwise in a credit line to the material. If material is not included in the article's Creative Commons licence and your intended use is not permitted by statutory regulation or exceeds the permitted use, you will need to obtain permission directly from the copyright holder. To view a copy of this licence, visit http://creativecommons.org/licenses/by/4.0/.

Introduction

One of the emerging issues jeopardizing the health of many individuals is lifestyle diseases. One such lifestyle disease which is affecting the global population is urolithiasis. Urolithiasis is a widespread condition with a wide range of undesirable aspects and causes, including dietary habits and other practices. A recent study revealed an increase in urolithiasis incidence in the global population since the year 1990 to the year 2019 by 48.57% [1]. Urolithiasis is a condition characterized by the formation of urinary tract calculi or stones. This condition includes the arrangement of calcifications in the urinary framework, generally in the kidneys or ureters, yet may likewise influence the bladder and additionally urethra. Uroliths are of different types, composed of calcium as calcium oxalate monohydrate and calcium hydrogen phosphate dihydrate, magnesium as ammonium magnesium phosphate hexahydrate, uric acid, and urates. Furthermore, cystine, hippuric acid, L-tyrosine, and xanthine also contribute to minute amounts of urolithic stone formation [2]. Of all urolith types calcium oxalate is the most common component (75%-90%) seen in uroliths.

The first and most important step in stone formation is crystallogenesis which takes place in three steps namely nucleation, growth, and aggregation. It is assumed that due to the excessive rate of excretions, the urine becomes saturated with insoluble materials, leading to the formation of crystals and aggregates to form a stone [3]. The increased oxidative stress causes Reactive oxygen species (ROS)-induced injury to the renal epithelial cells, damage, inflammation, and interacts with calcium oxalate crystals or oxalate ions leading to increased deposition of calcium oxalate crystals (kidney stones) [4, 5]. ROS are also produced when calcium oxalate stones erode the renal cells [6]. A high calcium level can stimulate the generation and release of intracellular ROS, which can increase the expression of matrix metalloproteinases (MMPs), which in turn are targets of Nuclear factor kappa-light-chain-enhancer of activated B cell (NF-κB), which may lead to the formation of kidney stones through a series of subsequent reactions [7].

The family of calcium-dependent-zinc-containing endopeptidases includes MMPs, which play a primary role in extracellular matrix remodeling [8]. MMPs like MMP-2 and MMP-9 are involved in the growth of renal stones by breaking through the basement membrane barriers in the urinary tract mainly by digesting collagen and fibronectin, [9]. NF-κB contains a family of nuclear transcription factors, which include p65 (RelA), RelB, c-Rel, NF-κB1, and NF-κB2 [10]. ROS activates NF-κB signaling, which, in turn, activates the expression of several NF-κB target genes [11]. Calcium oxalate crystals also activate the NF-κB signaling pathway and promote osteogenesis-related protein (OPN) expression in renal tubular epithelial cells [12]. The ROS/ NFκ-B/ MMP-9 signaling cascade thus targets MMP-9 downstream in urolithiasis [7]. By encouraging the transport of crystalline particles to the renal interstitium, MMP-9 may increase the formation of Randall's plaque and, subsequently kidney stone formation. Additionally, Randall's plaques may rupture due to MMP-9, allowing urine from the pelvis to come into contact with the hydroxyapatite and create the core of calcium salt deposition that causes kidney stone development [13]. In addition, it has been reported that abnormal MMP-9 and MMP-2 mediate renal fibrogenesis in stone-forming patients, which impairs kidney functions [14].

It is found that in renal tubular epithelial cells, a high calcium concentration stimulated calcium salt deposition and promoted the expression of MMP-9 which further promotes renal stone formation. Whereas silencing MMP-9 expression would inhibit the expression of the OPN, which would further inhibit calcium salt deposition, and eventually stone formation in the kidney. Similarly, when ROS were scavenged the expression of MMP-9, OPN, and RUNX2 (an osteogenic marker) was inhibited suggesting further inhibition of stone formation [7].

The human body is having an antioxidant defensive mechanism that is used to scavenge the ROS and protect the body from the development of oxidative stress-mediated diseases including kidney stones. Therefore, the therapeutic intervention of antioxidants helps to reduce oxidative stress/damage and the eventual crystal deposits [15]. Natural antioxidants like phenols and flavonoids were reported to mitigate free radical toxicity and alleviate stone formation in animal models as well as humans. Therefore, phytochemicals having antioxidant activities could be used in the treatment of kidney stones [16]. In addition, the antioxidant enzymes have also been found to be significant for urolithiasis management by preventing oxidative damage and showing protective effects on kidney stones. Antioxidant enzymes prevent calcium oxalate retention which could precipitate into kidney stones [17]. Glutathione S-transferase (GST), glutathione-disulfide reductase (GR), glutathione peroxidase (GPX), and superoxide dismutase (SOD) all play significant roles in maintaining a balance between ROS generation and breakdown in living organisms. Since none of these enzymes can eliminate all kinds of ROS on their own, they work together and synergistically to scavenge ROS [18]. The human calcium-sensing receptor (CaSR) controls the function of several tubular segments in the kidney by modulating electrolyte and water excretion. CaSR, in particular, inhibits proton and water excretion in collecting ducts, promotes phosphate absorption in proximal tubules, and decreases passive and active

calcium reabsorption in distal tubules. The usual balance of calcium, phosphate, protons, and water excretion may be disrupted in the renal medulla, by altered expression of the CaSR gene favouring stone development. As a result, It can be assumed to be a strong candidate gene for calcium nephrolithiasis [19].

Urolithiasis is a biochemical process with many steps and a high rate of recurrence. After urolithiasis treatment, there is a 50% possibility of stone development again in 7 years span whenever left untreated. Hence, the treatment of urolithiasis should include both curative as well as preventive therapy. As a result, proactive treatment is essential and recommended, particularly in stone former subjects [20]. Currently, for managing stone/calculus disruption locally, Surgical procedures, lithotripsy, and laparoscopy are employed. These procedures are costly and they eventually pose a risk of acute renal injury and even stone recurrence [21]. However, only a few medicinal plants and unique composite herbal formulations have been identified as an efficient treatment alternative for the minimally invasive prevention of renal calculi recurrence [22]. Utilizing these extracts could result in complementary and alternative medicine that could combat the drawbacks of modern pharmaceutical medications. In recent times, the hunt for new anti-lithiatic medicines from natural sources has assumed lesser significance. One of the plants which is used for the treatment of urinary calculi in the Indian traditional medicine system is *Ficus religiosa* [23].

The present study centers around the assessment of the antiurolithiatic capability of *F. religiosa* seeds considering, the promising results obtained from the phytochemical and antioxidant studies done until this point [24]. This study also aims to investigate possible mechanistic insights into the antiurolithiatic potential of relatively unexplored phytoconstituents of *F. religiosa* seeds. Based on the antioxidant potential of hexane, chloroform, ethyl acetate, and methanol extract of *F. religiosa* seeds, the seed extract with the highest activity was further evaluated for the volatile phytoconstituents by GC–MS analysis. Recently in vitro and in vivo absorption, distribution, metabolism, excretion, and toxicity (ADMET) prediction techniques have gained popularity, however, it is impossible to conduct intricate and pricey ADMET tests on a variety of chemicals [25]. As a Cost Saving High Throughput Alternative to Conventional Experimental Methods, in silico strategy to predict ADMET properties has become very attractive [26]. The GCMS evaluated phytoconstituents were then evaluated for their safety in ADMET while oral administration of the compound as a possible drug. Virtual screening is important in the identification of hits/leads against biological targets in computer-aided drug design and discovery as it saves time and money. Molecular docking is one of the virtual screening methods which is extensively used for this purpose. This strategy has successfully found the active molecules against the different targets [27].

Compounds from the ethyl acetate fraction of *F. religiosa* seeds, as reported in the GC–MS analysis were selected based on their drug-like properties through the Quantitative Estimate of Druglikeness (QED) score, and their non-violation of Lipinski rule of 5 by using the tool ADMET lab 2. The selected compounds were later docked to predict their binding potential against different biological targets (mentioned above) which were reported to be important in the management of kidney stone formation or urolithiasis as stated above. The biological targets studied include glycolate oxidase, glutathione-disulfide reductase, glutathione-S transferase, superoxide dismutase, glutathione peroxidase, Human calcium-sensing receptor, and MMP-9 and MMP-2.

Traditionally, *F. religiosa* has been reported to have antioxidant potential, prevent stone formation, and bear protective effects to prevent kidney cell damage and is used for its diuretic and anti-urolithiasis activity [28]. However, there are currently no reports indicating which phytochemicals are specifically responsible for this plant's anti-urolithiasis activity. This is the first kind of report of individual phytochemicals of *F. religiosa* seeds that were investigated against multiple targets responsible for urolithiasis or kidney stone.

Materials and methods

Plant material collection

F. religiosa figs were gathered from the region, which is located at 17° 43′ 47.3880" N and 83° 19′ 17.3820" E. Seeds were isolated from figs physically and cleaned. A mechanical blender of laboratory quality was used to grind the cleaned seeds into a fine powder after they had been shade dried. To get uniform-sized particles this seed powder was then sieved through a fine sieve. The seed powder was again shade dried to get rid of any moisture retained during the grinding process. The dried seed powder was stored in airtight containers at room temperature in an aseptic environment for the subsequent extraction process.

Preparation of extract

F. religiosa seeds were then extracted by Soxhlet extraction method using different solvents successively in order of their increasing polarities (hexane: 0.1, followed by chloroform: 4.1, then ethyl acetate: 4.4, and then methanol: 5.1). The 450 g of *F. religiosa* seed powder were first extracted in hexane at 70 °C, the residue from the hexane extraction was then extracted using the Soxhlet apparatus for 14 h in chloroform at 61.2 °C, followed by

ethyl acetate at 77 °C, and methanol at 64.7 °C. The seed extracts obtained were subsequently concentrated by distillation, which involved evaporating the solvent. The concentrated extracts were then dried and kept in a desiccator at room temperature for further investigation. The aqueous extract was prepared by taking 10 g of *F. religiosa* seed powder mixed with 100 ml of distilled water, which was then agitated for 10 min with a magnetic stirrer, and then boiled for 30 min at 80 °C. Whattmann Filter Paper No. 1 was used to filter this aqueous extract and stored at -4 °C for further use.

In vitro free radical scavenging activity

Reducing power assay

The approach outlined by [29] was used to assess the extracts' reducing power ability. The plant sample was dissolved in dimethyl sulfoxide (DMSO) to obtain various concentrations, 100 µg/ml, 200 µg/ml, 300 µg/ml, 400 µg/ml, and 500 µg/ml in several reaction tubes. 1.0 ml of varied plant extract concentrations, 2.5 ml of 0.2 M sodium phosphate buffer, and 2.5 ml of 1% potassium ferricyanide made up the reaction mixture. After 30 min of incubation at 50 °C, the reaction was stopped by adding 2.5 ml of 10% trichloroacetic acid and centrifuging the liquid for 10 min at 3000 rpm. After centrifugation 2.5 ml of the upper layer was combined with double distilled water and 0.1% ferric chloride. The absorbance was measured at 700 nm against a blank that was made up entirely of double distilled water as opposed to plant extract. As standards, butylated hydroxytoluene (BHT) and ascorbic acid were used. An increase in absorbance implies that the sample has more reducing power. The results were expressed as ascorbic acid equivalents obtained from the standard curve of ascorbic acid with a regression equation of $y = 0.0063x—0.0008$.

Hydroxyl radical scavenging assay

The extracts' capacity to scavenge hydroxyl radicals was assessed using the procedure described by Klein et al. [30]. The reaction mixture contained 1.0 ml of extracts dissolved in Dimethyl sulfoxide (DMSO) at various concentrations (100 µg/ml, 200 µg/ml, 300 µg/ml, 400 µg/ml, and 500 µg/ml), 1.0 ml of iron- Ethylenediaminetetraacetic acid (EDTA) solution (0.13% ferrous ammonium sulfate and 0.26% EDTA), 0.5 ml of 0.018% EDTA, 1.0 ml of DMSO (0.85% in 0.1 M phosphate buffer pH7.4) and 0.5 ml of 0.22% ascorbic acid. After 15 min of heating in a water bath at 80–90 °C with tight-fitting caps on the tubes, the reaction was stopped by adding 1.0 ml of 17.5% ice-cold Trichloroacetic Acid (TCA). To this reaction mixture, 3.0 ml of Nash reagent (a mixture of 75.0 g of ammonium acetate, 3.0 ml of glacial acetic acid, 2.0 ml of acetylacetone, and distilled water to make up the final volume to 1 L) was added and kept at room temperature for 15 min for colour development. At 412 nm, the intensity of the generated yellow colour was assessed in comparison to a reagent blank. As a control, the reaction mixture without the sample was employed. BHT and ascorbic acid were employed as benchmarks. The following formula was used to determine the percentage of hydroxyl radical scavenging activity (HRSA):

$$\% \, HRSA = [(control\ OD - sample\ OD) \div controlOD] \times 100$$

Estimation of reduced glutathione

The Boyne and Ellman technique [31] was used to determine the quantity of reduced glutathione (GSH) present in the samples. 4.0 ml of the metaphosphoric acid precipitating solution (1.67 g of glacial metaphosphoric acid, 0.2 g EDTA, and 30 g NaCl mixed in 100 ml water) was added to 1 ml of the sample extract dissolved in DMSO at various concentrations (100 µg/ml, 200 µg/ml, 300 µg/ml, 400 µg/ml, and 500 µg/ml) and centrifuged. After centrifugation, 2.0 ml of the protein-free supernatant was combined with 1.0 ml of 5,5′-dithiobis-(2-nitrobenzoic acid (DTNB) reagent (40 mg of DTNB was dissolved in 100 ml of aqueous 1% trisodium citrate), and0.2 ml of 0.4 M Na_2HPO_4. Within 2 min, the absorbance was measured at 412 nm. The amount of GSH was given as nmol/ml using a standard glutathione curve having a regression equation of $y = 0.0049x + 0.0014$.

GC–MS analysis

Sample preparation

100 µg of *F. religiosa* ethyl acetate seed extract was dissolved in 1 ml of methanol solvent. A vortex stirrer was used to swirl this dissolved solution before it was filtered using a 0.2-micron membrane syringe filter. The clear extract was then used for analysis using gas chromatography along with a mass spectrometry (GC–MS) system.

Chromatography run

The Shimadzu QP 2010 Ultra GC- MS instrument from Agilent Technologies was used for the GC- MS analysis of the ethyl acetate seed extract from *F. religiosa*. A volume injection of 1µL was used to inject a DB- 5MS, 5 phenyl methyl siloxane column having an inner diameter (ID) of 30 m and a film thickness of 0.25 m. A standard injection mode auto-sampler from Agilent, Santa Clara, USA, was used. Helium is used as the carrier gas with an inflow of 1.0 ml/ min. The oven temperature was originally programmed at 70 °C and held for 5 min, further gradually raised to 310 °C, and further held for 10 min while the injector was operated at 250 °C. After that, the sample was eventually eluted using a gradient that ran for 63 min. After a 4.5-min

solvent delay, full scan and monitoring mode were used to acquire mass spectra in the 50–700 m/z range. Between the spectrum of the unknown component of the ethyl acetate extract of *F. religiosa* seeds and the spectra of the known components kept in the NIST, WELLY, and TOX libraries, a comparison was done. Each phytochemical in the plant extract was named and its molecular weight and structure were determined using the data stored in libraries.

Pharmacokinetic analysis and drug-likeness prediction

To overcome the unfavorable effects of a drug candidate at the beginning of the drug development process, it is essential to determine the ADMET (absorption, distribution, metabolism, excretion, toxicity) features. Online prediction models were created that were effective and precise for the in-silico estimate of ADMET parameters. To calculate ADMET features such as absorption, distribution, metabolism, excretion, toxicity, and physicochemical properties of all drugs, the online in-silico prediction model ADMET lab 2.0 was utilized. All GC–MS Quantified Phytoconstituents were converted to Simplified Molecular Input Line Entry System (SMILES) format using PubChem and were then submitted to the ADMETlab 2.0 web server.

Physicochemical characteristics, QED score, gastrointestinal tract absorption, blood–brain barrier (BBB), fraction unbound in plasma (Fu, P), the volume of distribution (VD), CYP3A4 substrate, CYP3A4 inhibitor, Clearance, Rat Oral Acute Toxicity, and Acute Toxicity Rule were all considered while determining ADMET factors.

Docking studies

For Autodocking analysis of the chosen ligands against selected target proteins, the AutoDock Vina tool provided by the SeamDock web server (https://bioserv.rpbs.univ-paris-diderot.fr/services/SeamDock/) was used [32]. An open-source Python library, Docking_py is a simple and unified library, which was optimized by Jupyter Notebooks, and it was used to construct the AutoDock Vina tool in the SeamDock web server. The ligand was uploaded in SMILES format, which is converted to pdb format using RDKit. The ligand pdb file is then processed using the prepare_ligand4.py (MGL tools). Where this program automatically computes the atomic charge, assigns atom types, repairs missing hydrogen atoms, and however torsions of the ligand will be kept active, and the output is a pdbqt file which will be used as an input file AutoDock Vina tool. Receptor structure docking grid parameters can be prepared by using MGLTools preprare_gpf4.py. The visualization of docking results in 3D mode was facilitated by the NGLview library.

Statistical analysis

Each extraction method and the antioxidant study were carried out triple, and statistical analysis was carried out individually for each test. Three parallel replicates' means and standard error mean (SEM) were used to express the results. Using Microsoft Excel 2022, a one-way analysis of variance (ANOVA) with the Tukey test of multiple comparisons was conducted for each report. The cutoff for statistical significance was $p \leq 0.05$.

Results

Reducing power assay

Figure 1a provides a summary of each *F. religiosa* seed extract's reducing power ability in terms of ascorbic acid equivalents at various concentrations (100 µg/ml, 200 µg/ml, 300 µg/ml, 400 µg/ml, and 500 µg/ml) in comparison to standards (ascorbic acid and BHT). All extracts showed a linear increase in activity with increasing concentrations. Of all the extracts tested the highest activity was found for ethyl acetate extract at a concentration of 500 µg/ml (111.22 ± 0.06), which is lower than that of standard ascorbic acid (362.80 ± 1.85 g/ml) and BHT (259.95 ± 0.11 g/ml) at the same concentration (500 µg/ml). The analysis of the cumulative reducing power capacity for all concentrations of different *F. religiosa* seed extracts and standards revealed that the Ethyl acetate extract exhibited the highest activity (90.68 ± 0.097 µg/ml), although lower than that of the standard's ascorbic acid (244.67 ± 0.716 µg/ml) and BHT (184.37 ± 0.126 µg/ml). This analysis looked at the cumulative reducing power ability of all concentrations of different *F. religiosa* seed extracts and standards. These total data were examined using an F-statistic, [$F(6,14) = 60527.20$, $p < 0.05$], as shown in Fig. 1d.

Hydroxyl radical scavenging assay

Figure 1b depicts a summary of each *F. religiosa* seed extract's percentage hydroxy radical scavenging activity at various concentrations (100 µg/ml, 200 µg/ml, 300 µg/ml, 400 µg/ml, and 500 µg/ml) in comparison to standards (ascorbic acid and BHT). Each extract showed increased activity with an increase in concentration. At the highest concentration (500 µg/ml) methanol extract showed the highest activity (90.55 ± 0.07%) which is greater than that of ascorbic acid (85.56 ± 0.29%) but slightly lower than BHT (93.31 ± 0.37%). However, the cumulative percentage inhibitions for all concentrations of different *F. religiosa* seed extracts and standards revealed that the Ethyl acetate extract exhibited the highest activity in terms of percentage of inhibition (79.87 ± 0.187%). This value was higher than that of the standard ascorbic acid (74.03 ± 0.387%) but lower than that of BHT (88.29 ± 0.257%). The cumulative results

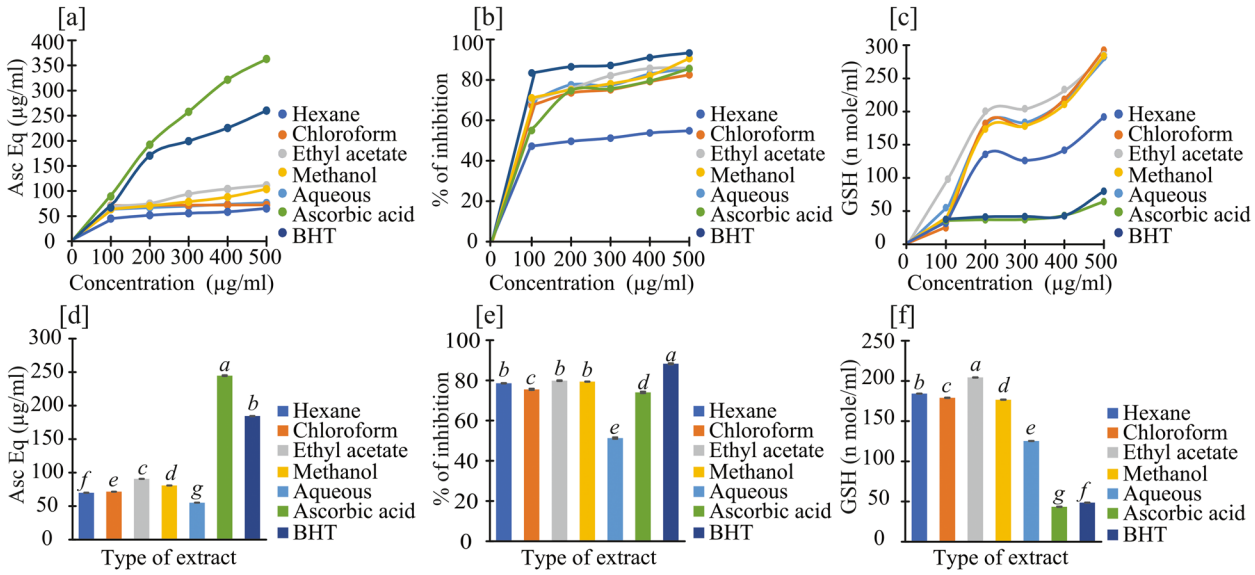

Fig. 1 **a** Reducing power ability at different concentrations, **b** % hydroxy radical scavenging activity at different concentrations, **c** Total reduced glutathione at different concentrations, **d** Cumulative reducing power ability of different seed extracts, **e** Cumulative % hydroxy radical scavenging activity of different seed extracts, **f** Cumulative total reduced glutathione of different seed extracts of *F. religiosa*. The results were expressed as Mean ± SEM; $N = 3$. Tukey test values labelled with different letters are significantly different at $p \leq 0.05$

were analyzed using an F-statistic [$F(6,14) = 1774.515$, $p < 0.05$], as depicted in Fig. 1e.

Estimation of reduced glutathione

Figure 1c summarises the total reduced glutathione in nanomoles/millilitre (nmol/ml) of all *F. religiosa* seed extracts at various concentrations (100 µg/ml, 200 µg/ml, 300 µg/ml, 400 µg/ml, and 500 µg/ml) in comparison to standards (ascorbic acid and BHT). The amount of total reduced glutathione increased as the concentration of each extract was increased. At the highest concentration (500 µg/ml) of all extracts assayed, ethyl acetate extract exhibited the highest amount of reduced glutathione (285.84 ± 0.21 nmol/ml) which is much higher than the standard ascorbic acid (64.20 ± 0.20 nmol/ml) and BHT (79.92 ± 0.42 nmol/ml). Likewise, the cumulative activity for all concentrations of different *F. religiosa* seed extracts was analyzed, revealing that the ethyl acetate extract exhibited the highest amount of reduced glutathione (204.37 ± 0.162 nmol/ml) among the seed extracts. This value was higher than that of the standard's ascorbic acid (43.44 ± 0.219 nmol/ml) and BHT (48.64 ± 0.170 nmol/ml). These cumulative results were analyzed using an F-statistic [$F6,14) = 134006.7956$, $p < 0.05$], as depicted in Fig. 1f.

GC–MS analysis

The results of in-vitro antioxidant assays of the evaluated hexane, chloroform, ethyl acetate, methanol, and aqueous *F. religiosa* seed extracts revealed that ethyl acetate extract is the most potent of all. Hence, to determine the underlying phytoconstituent that might be responsible for the antioxidant assay, *F. religiosa* seed ethyl acetate extract was analyzed using gas chromatography along with mass spectrometry. Figure 2 displays the GC–MS intensities of the *F. religiosa* ethyl acetate extract's GC–MS chromatogram. 62 peaks were seen in the ethyl acetate crude extracts of the *F. religiosa* seeds GC–MS chromatogram. Of these 62 peaks, some compounds formed multiple peaks at different retention times. Hexadecan-1-ol gave two peaks at retention times 20.060, and 25.398 likewise, Hexadecane gave two peaks at retention times 22.674, and 25.582, and Pentadecanoic acid gave 2 peaks at 29.739, and 32.103, Pentadecanoic acid methyl ester gave two peaks at 30.118, and 30.984, docosan-1-ol gave two peaks at 30.280 and 30.994, Hexadecanoic acid, methyl ester gave two peaks at 32.473, and 33.402, Heptadecanoic acid, methyl ester gave two peaks at 34.837, and 35.727, pentatriacontane gave three peaks at 42.611, 45.444, and 51.713. Hence, we can say that 53 different compounds were identified from ethyl acetate crude extracts of the *F. religiosa* seeds. Although all the compounds belonged to different classes, the most abundant compounds were fatty acid methyl esters (29.03%), hydrocarbons (14.51%), fatty alcohols (14.51%), phenols (11.29%), fatty acids (6.45%), and all others were less abundant in the extract. In Table 1, the discovered compounds' retention times, molecular formula, molecular

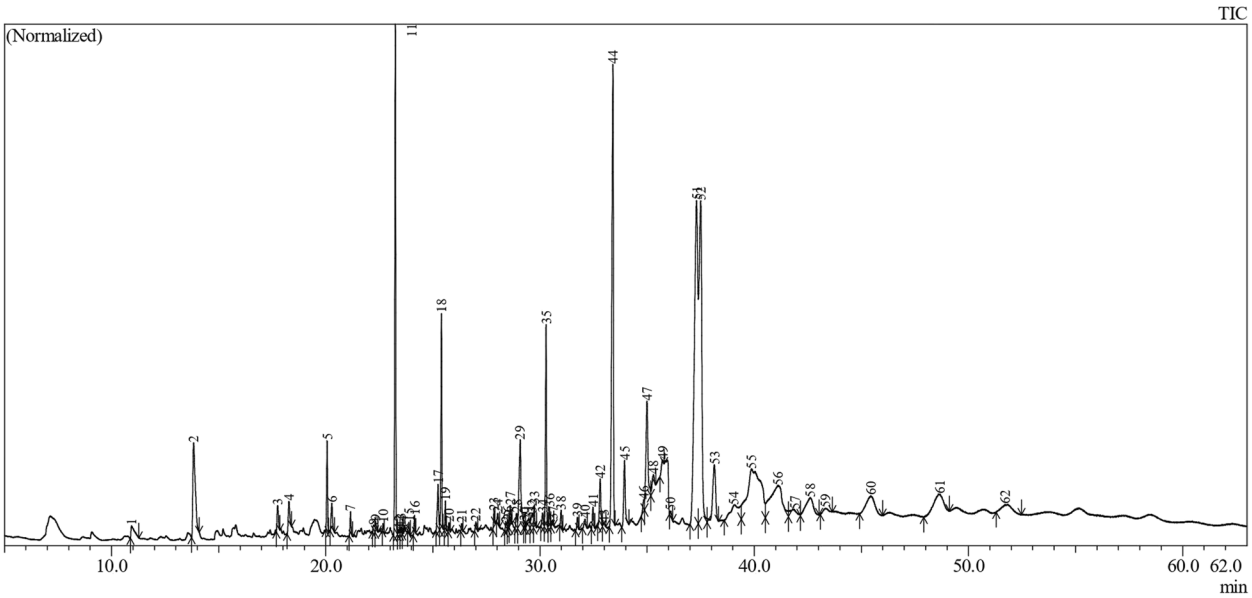

Fig. 2 **a** GC–MS chromatogram of *F. religiosa* seed ethyl acetate extract

weight, peak area, and chemical class are displayed. Based on the peak area most abundant compounds found in the evaluated extract in order of their abundance is ethyl (9Z,12Z)-octadeca-9,12-dienoate (15.46%), methyl (E)-octadec-9-enoate (12.87%), methyl hexadecanoate (9.84%), octacosan-1-ol (9.24%).

Pharmacokinetic analysis and drug-likeness prediction

GCMS-evaluated compounds were sufficiently advanced to be considered oral drug candidates. And hence, structural or physicochemical inspections were done to determine the drug-likeness of these compounds using the ADMETLAB2.0 online tool (https://admetmesh.scbdd.com/service/evaluation/index). ADMET analysis evaluated Drug-likeness, pharmacokinetics, and physicochemical characteristics. "Drug-likeness" evaluates qualitatively if a molecule has a probability of developing into an oral medication in terms of bioavailability. The results of the ADMET analysis of the 53 compounds are summarised in Table 2. The medicinal chemistry of the 53 compounds identified by GCMS analysis was evaluated based on 2 factors if they follow Lipinski's rule of 5 and their QED score. Absorption studies of these 53 compounds revealed that 16 compounds had low gastrointestinal absorption and 37 compounds had high gastrointestinal absorption. Distribution studies of the above 53 compounds were studied based on volume distribution, BBB penetration, and Fu, P. VD values of these compounds ranged from 0.221 L/Kg to 8.866 L/Kg.

Of all compounds evaluated, 30 compounds showed excellent BBB penetration, 15 had medium BBB penetration, and 8 had low BBB penetration. The Fu, *P* values of these compounds ranged from 0.12% to 77.664%. Metabolic studies were done on these compounds based on whether the given compound is a substrate or inhibitor of the CYP3A4 enzyme of the human cytochrome P450 family. Out of 53, 47 compounds are neither substrates nor inhibitors of CYP3A4. 3,5-Di-tert-butyl phenol is both substrate as well as inhibitor, 2,5-ditert-butylbenzene-1,4-diol and N-[[3,6-dichloro-2,7-bis[2-(diethylamino)ethoxy]fluoren-9-ylidene]amino]-2,2-dimethylpropanamide are noninhibitors but substrate, 7,9-ditert-butyl-1-oxaspiro[4.5]deca-6,9-diene-2,8-dione; ethyl (9Z,12Z)-octadeca-9,12-dienoate and methyl (E)-octadec-9-enoate and methyl (E)-octadec-9-enoate are inhibitors but non substrate.

The excretory properties of the above 53 compounds were analyzed based on their clearance value. 29 compounds had good clearance values which is above 5 ml/min/kg and the rest 24 compounds had poor clearance values which is below 5 ml/min/kg. The toxicology of these compounds was studied based on rat oral acute toxicity and acute toxicity rule. All the analyzed compounds had low toxicity based on rat oral acute toxicity studies except for 2 compounds which were highly toxic and 3 were medium toxic. But, according to the acute toxicity rule, none of the compounds were toxic. Based on the ADMET analysis of all 53 compounds, 6 compounds having the highest QED score, good absorption, good clearance, and low toxicity were chosen to be the best of all. These compounds are 2-Methoxy-4-vinylphenol; 3,5-Di-tert-butylphenol; diethyl benzene-1,2-dicarboxylate; 4-hydroxy-3,5-dimeth-

Table 1 Compounds identified from *F. religiosa* seed ethyl acetate extract using GC–MS analysis

Peak no	CN	MF	MW (g/mol)	RT	Area%	CC
1	Methyl 3-hydroxytetradecanoate	$C_{15}H_{30}O_3$	258.4	10.93	0.6	Fatty acid methyl ester
2	Naphthalene	$C_{10}H_8$	128.17	13.83	3.18	Aromatic hydrocarbon
3	2-Methoxy-4-vinylphenol	$C_9H_{10}O_2$	150.17	17.75	0.47	Phenol
4	tert-Butyldimethylsilyl acetate	$C_8H_{18}O_2Si$	174.31	18.28	0.62	Fatty acid
5	hexadecan-1-ol	$C_{16}H_{34}O$	242.44	20.06	1.12	Fatty alcohol
6	1-Bromo-2-methyldecane	$C_{11}H_{23}Br$	234.1	20.28	0.55	Hydrocarbon
7	Nonanoic acid, 9-oxo-, methyl ester	$C_{10}H_{18}O_3$	186.25	21.15	0.32	Fatty acid methyl ester
8	Ethyl(dimethyl)ethoxysilane	$C_6H_{16}OSi$	132.28	22.22	0.14	Alkyl substituted silane
9	Butanoic acid, 3-methyl-, hexadecyl ester	$C_{21}H_{42}O_2$	326.6	22.32	0.2	Fatty acid methyl esters
10	Hexadecane	$C_{16}H_{34}$	226.44	22.67	0.1	Hydrocarbon
11	3,5-Di-tert-butylphenol	$C_{14}H_{22}O$	206.32 g/mol	23.25	6.72	phenol
12	3,7,11-Trimethyl-1-dodecanol	$C_{15}H_{32}O$	228.41	23.42	0.08	Fatty alcohol
13	Tricyclo[5.2.1.02,6]dec-3-en-8-ol	$C_{10}H_{14}O$	150.22	23.52	0.11	Cyclic alcohol
14	Dodecanoic acid, methyl ester	$C_{13}H_{26}O_2$	214.34	23.6	0.04	Fatty acid methyl ester
15	1-iododotriacontane	$C_{32}H_{65}I$	576.76	23.88	0.14	Iodo alkane
16	Dimethyl nonanedioate	$C_{11}H_{20}O_4$	216.27	24.14	0.23	Fatty acid methyl ester
17	Diethyl benzene-1,2-dicarboxylate	$C_{12}H_{14}O_4$	222.24	25.24	0.82	Benzoic acid ester
18	Hexadecan-1-ol	$C_{16}H_{34}O$	242.44	25.4	2.62	Fatty alcohol
19	Hexadecane	$C_{16}H_{34}$	226.44	25.58	0.33	Hydrocarbon
20	1-Tetradecyl acetate	$C_{16}H_{32}O_2$	256.42	25.75	0.1	Fatty acid ester
21	Diphenylmethanone	$C_{13}H_{10}O$	182.22	26.35	0.1	Benzophenone
22	4-hydroxy-3,5-dimethoxybenzaldehyde	C_9H10O_4	182.17	27.01	0.17	Methoxy phenols
23	n-Tridecan-1-ol	$C_{13}H_{28}O$	200.36	27.85	0.18	Fatty alcohol
24	Tetracosane	$C_{24}H_{50}$	338.7	28.02	0.16	Hydrocarbon
25	2-hexadecyloxirane	$C_{18}H_{36}O$	268.48	28.4	0.13	Epoxide ether
26	2,5-ditert-butylbenzene-1,4-diol	$C_{14}H_{22}O_2$	222.32 g/mol	28.5	0.11	Phenol
27	Methyl 12-methyltridecanoate	$C_{15}H_{30}O_2$	242.4	28.61	0.3	Fatty acid methyl ester
28	(E)-3-(4-methoxyphenyl)prop-2-enoic acid	$C_{10}H_{10}O_3$	178.18	28.9	0.28	Hydroxyphenolics
29	1-butylsulfanyl-4-methylbenzene	$C_{11}H_{16}S$	180.31	29.08	2.43	Phenyl derivative
30	1-bromooctadecane	$C_{18}H_{37}Br$	333.4	29.27	0.13	Bromo alkane
31	2-nitrobenzene-1,3-diol	$C_6H_5NO_4$	155.11 g/mol	29.46	0.32	phenol
32	2-methoxy-4-prop-2-enylphenol	$C_{10}H_{10}O_2$	164.2 g/mol	29.62	0.43	phenol
33	Pentadecanoic acid	$C_{15}H_{30}O_2$	242.4	29.74	0.34	Fatty acid
34	methyl pentadecanoate	$C_{16}H_{32}O_2$	256.42	30.12	0.24	Fatty acid methyl ester
35	docosan-1-ol	$C_{22}H_{46}O$	326.6	30.28	2.82	Fatty alcohol
36	Henicosane	$C_{21}H_{44}$	296.6	30.43	0.29	Hydrocarbon
37	2-hexyldecan-1-ol	$C_{16}H_{34}O$	242.44	30.59	0.09	Fatty alcohol
38	methyl pentadecanoate	$C_{16}H_{32}O_2$	256.42	30.98	0.25	Fatty acid methyl ester
39	Bis(2-methylpropyl) benzene-1,2-dicarboxylate	$C_{16}H_{22}O_4$	278.34 g/mol	31.75	0.2	Phthalate Esters
40	Pentadecanoic acid	$C_{15}H_{30}O_2$	242.4	32.1	0.21	Fatty acid
41	Methyl hexadecanoate	$C_{17}H_{34}O_2$	270.5	32.47	0.36	Fatty acid methyl ester
42	7,9-ditert-butyl-1-oxaspiro[4.5]deca-6,9-diene-2,8-dione	$C_{17}H_{24}O_3$	276.4	32.81	0.93	Diketone
43	Tetrapentacontane	$C_{54}H_{110}$	759.4	33	0.09	Hydrocarbon
44	Methyl hexadecanoate	$C_{17}H_{34}O_2$	270.5	33.4	9.84	Fatty acid methyl ester
45	Dibutyl benzene-1,2-dicarboxylate	$C_{16}H_{22}O_4$	278.34 g/mol	33.94	1.48	Phthalate Esters
46	Methyl heptadecanoate	$C_{18}H_{36}O_2$	284.5	34.84	0.23	Fatty acid methyl ester
47	Docosan-1-ol	$C_{22}H_{46}O$	326.6	34.99	3	Fatty alcohol
48	Tetracontane-1,40-diol	$C_{40}H_{82}O_2$	595.1	35.29	0.49	Fatty alcohol
49	Methyl heptadecanoate	$C_{18}H_{36}O_2$	284.5	35.73	0.21	Fatty acid methyl ester

Table 1 (continued)

Peak no	CN	MF	MW (g/mol)	RT	Area%	CC
50	Methyl 2-hydroxyhexadecanoate	$C_{17}H_{34}O_3$	286.4 g/mol	36.1	0.1	Fatty acid methyl ester
51	Ethyl (9Z,12Z)-octadeca-9,12-dienoate	$C_{20}H_{36}O_2$	308.5	37.31	15.46	Fatty acid methyl ester
52	Methyl (E)-octadec-9-enoate	$C_{19}H_{36}O_2$	296.5 g/mol	37.5	12.87	Fatty acid methyl ester
53	Methyl octadecanoate	$C_{19}H_{38}O_2$	298.5	38.14	2.34	Fatty acid methyl ester
54	Methyl 10-methyloctadecanoate	$C_{20}H_{40}O_2$	312.5	39.04	1.82	Fatty acid methyl ester
55	Octacosan-1-ol	$C_{28}H_{58}O$	410.8	39.87	9.24	Fatty alcohol
56	Octadecanoic acid	$C_{18}H_{36}O_2$	284.5	41.11	5.23	Fatty acid
57	(Z)-hexadec-7-enal	$C_{16}H_{30}O$	238.41	41.88	0.63	Aldehyde
58	Pentatriacontane	$C_{35}H_{72}$	492.9	42.61	1.76	Hydrocarbon
59	Methyl icosanoate	$C_{21}H_{42}O_2$	326.6	43.34	0.34	Fatty acid methyl ester
60	Pentatriacontane	$C_{35}H_{72}$	492.9	45.44	2.14	Hydrocarbon
61	N-[[3,6-dichloro-2,7-bis[2-(diethylamino)ethoxy]fluoren-9-ylidene]amino]-2,2-dimethylpropanamide	$C_{30}H_{42}Cl_2N_4O_3$	577.6	48.65	2.55	Fatty acid amide
62	Pentatriacontane	$C_{35}H7_2$	492.9	51.71	1.22	Hydrocarbon

CN Compound name, *MF* Molecular formula, *MW* Molecular weight, *RT* Retention time, *CC* Chemical Class

oxybenzaldehyde; 2-methoxy-4-prop-2-enylphenol; and bis(2-methylpropyl) benzene-1,2-dicarboxylate.

Docking analysis

In the current study, seven target proteins namely (1) Glutathione-disulfide reductase (PDB ID: 1BWC), (2) Glutathione-S-transferase (PDB ID: 4MPG), (3) Superoxide dismutase (PDB ID: 1CB4), (4) Glutathione peroxidase (PDB ID: 2WGR), (5) Human calcium-sensing receptor (PDB ID: 5FBH), (6) Matrix metalloproteinase (MMP)-9 (PDB ID: 4XCT) and (7) MMP2 (PDB ID: 1ck7) were docked with 6 ligands, namely (L-I) 2-Methoxy-4-vinylphenol (PubChem CID: 332), (L-II) 3,5-Di-tert-butylphenol (PubChem CID: 70825), (L-III) diethyl benzene-1,2-dicarboxylate (PubChem CID: 6781), (L-IV) 4-hydroxy-3,5-dimethoxybenzaldehyde (PubChem CID: 8655), (L-V) 2-methoxy-4-prop-2-enylphenol (PubChem CID: 13245), (L-VI) bis(2-methyl propyl) benzene-1,2-dicarboxylate (PubChem CID: 3314) and the results are depicted in Table 3.

The box coordinates for the target protein 1 were -3×-8×-7 Å (center) and 63×63×67 Å (size). The ligand L-II yielded the highest ΔG for the target protein 1, which was about -6.4 kcal/mol in comparison with other ligands. L-II has shown hydrophobic and hydrogen bonding toward target protein 1. The oxygen atom O1 of L-II was involved in hydrogen bonding with amino acids Asp363, Asn365, and Lys452, whereas carbon atoms C3 is involved in hydrophobic contact with amino acid Lys452, likewise, C4 with Pro368 and Ala448, C8 with Ile367, C12 with Ile367, Val341, Leu362, C13 with Ala344 and C14 with Ile367. In this interaction, Lys452 is involved in both hydrogen bonding and hydrophobic interactions (Fig. 3a).

The box coordinates for the target protein 2 were -3×-1×-2 Å (center) and 57×49×59 Å (size). The ligand, L-II yielded the highest ΔG for the target protein 2, which was about -6.9 kcal/mol in comparison with other ligands. L-II has shown hydrophobic contact, hydrogen bonding, and weak hydrogen bonding toward target protein 2. The oxygen atom O1 of L-II was involved in hydrogen (H) bonding with amino acids His40, whereas C14, C8, C6, C10, C3, C13, C13, and C13 were involved in hydrophobic contact with amino acids Val10, Leu35, Leu35, Leu35, Lys53, Leu114, Trp115, Leu119, respectively (Fig. 3b).

The box coordinates for the target protein 3 were 0×1×1 Å (center) and 44×71×44 Å (size). The ligand, L-II yielded the highest ΔG for the target protein (3), which was about -6.2 kcal/mol in comparison with other ligands. L-II has shown hydrophobic contact and hydrogen bonding toward target protein 3. The oxygen atom O1 of L-II was involved in hydrogen (H) bonding with amino acids Val7 and Cys144. Whereas carbon atoms of L-II, C3, C13, C10, C1, C13, and C12 were involved in hydrophobic contact with amino acids Val7, Val146, Lys9, Asn51, Val146, Val146, respectively (Fig. 3c).

The box coordinates for the target protein 4, Glutathione peroxidase were -1×1×2 Å (center) and 40×44×52 Å (size). The L-III and L-IV yielded the highest ΔG for the target protein 4, which was about -5.1 kcal/mol in comparison with other ligands. L-III and L-IV have shown hydrophobic contact, hydrogen bonding, and weak hydrogen bonding toward target protein 4. For L-III, oxygen atom O2 is involved in hydrogen binding

Table 2 Computed parameter values of *F. religiosa* phytochemicals by using ADMETLAB-2.0

S.no	Compound Name	QED score	Violations of Lipinski	GI Absorption	Volume distribution	Fraction unbound in plasms	BBB	CYP3A4	Clearance	Rat Oral Acute Toxicity	Acute Toxicity Rule
1	Methyl 3-hydroxytetradecanoate	0.427	0	High	0.648	4.146% L	Poor	NI/NS	9.612	Low	0
2	Naphthalene	0.511	0	Low	1.177	5.173% H	Poor	NI/NS	10.472	Low	0
3	2-Methoxy-4-vinylphenol	0.699	0	High	0.918	11.299% H	Medium	NI/NS	13.581	Medium	0
4	tert-Butyldimethylsilyl acetate	0.571	0	High	1.478	7.539% H	Excellent	NI/NS	3.348	Low	0
5	Hexadecan-1-ol	0.401	0	High	2.697	1.643% L	Excellent	NI/NS	5.716	Low	0
6	1-Bromo-2-methyldecane	0.42	0	Low	3.552	2.603% L	Poor	NI/NS	3.277	Medium	0
7	Nonanoic acid, 9-oxo-, methyl ester	0.331	0	High	0.657	77.664% H	Poor	NI/NS	7.75	Low	0
8	Ethyl(dimethyl)ethoxysilane	0.535	0	High	1.051	1.532% L	Excellent	NI/NS	5.07	Low	0
9	Butanoic acid, 3-methyl-, hexadecyl ester	0.211	1	Low	2.409	1.772% L	Excellent	NI/NS	6.265	Low	0
10	Hexadecane	0.315	1	Low	3.848	1.584% L	Excellent	NI/NS	4.564	Low	0
11	3,5-Di-tert-butylphenol	0.68	0	High	4.514	6.813% H	Medium	I/S	7.521	Low	0
12	3,7,11-Trimethyl-1-dodecanol	0.577	0	High	1.74	2.439% L	Medium	NI/NS	9.13	Low	0
13	Dicyclopentenyl alcohol	0.52	0	High	0.947	30.305% H	Medium	NI/NS	11.803	Medium	0
14	Dodecanoic acid, methyl ester	0.404	0	High	0.813	3.435% L	Poor	NI/NS	6.514	Low	0
15	1-iododotriacontane	0.045	2	Low	5.569	0.48% L	Excellent	NI/NS	4.091	Low	0
16	Dimethyl nonanedioate	0.46	0	High	0.615	55.639% H	Poor	NI/NS	9.464	Low	0
17	Diethyl benzene-1,2-dicarboxylate	0.731	0	High	1.316	9.509% H	Excellent	NI/NS	12.247	Low	0
18	1-Tetradecyl acetate	0.332	0	High	1.601	2.654% L	Medium	NI/NS	3.256	Low	0
19	Diphenylmethanone	0.652	0	High	0.658	1.674% L	Excellent	NI/NS	1.416	Low	0
20	4-hydroxy-3,5-dimethoxybenzaldehyde	0.714	0	High	0.646	16.177% H	Poor	NI/NS	8.824	Low	0
21	n-Tridecan-1-ol	0.493	0	High	2.106	2.454% L	Medium	NI/NS	6.843	Low	0
22	Tetracosane	0.183	1	Low	4.766	1.048% L	Excellent	NI/NS	4.412	Low	0
23	2-hexadecyloxirane	0.252	0	Low	1.802	1.611% L	Excellent	NI/NS	4.237	Low	0
24	2,5-ditert-butylbenzene-1,4-diol	0.657	0	High	4.41	5.181% H	Excellent	NI/S	7.773	Low	0
25	Methyl 12-methyltridecanoate	0.387	0	High	0.891	2.152% L	Medium	NI/NS	6.444	Low	0
26	(E)-3-(4-Methoxyphenyl)prop-2-enoic acid	0.718	0	High	0.221	8.527% H	Medium	NI/NS	4.341	Low	0
27	1-butylsulfanyl-4-methylbenzene	0.5	0	High	2.614	3.858% L	Poor	NI/NS	10.637	Low	0
28	1-bromooctadecane	0.201	1	Low	4.053	1.534% L	Excellent	NI/NS	3.128	Low	0
29	2-nitrobenzene-1,3-diol	0.468	0	High	0.467	9.843% H	Excellent	NI/NS	8.828	High	0
30	2-methoxy-4-prop-2-enylphenol	0.693	0	High	0.833	3.220% L	Excellent	NI/NS	14.042	Low	0
31	Pentadecanoic acid	0.453	0	High	0.514	1.117% L	Excellent	NI/NS	2.343	Low	0
32	Methyl pentadecanoate	0.332	0	High	1.69	1.628% L	Medium	NI/NS	5.197	Low	0
33	Docosan-1-ol	0.226	1	Low	3.657	1.339% L	Excellent	NI/NS	5.114	Low	0
34	Henicosane	0.223	1	Low	4.419	1.246% L	Excellent	NI/NS	4.482	Low	0

Table 2 (continued)

S.no	Compound Name	QED score	Violations of Lipinski	GI Absorption	Volume distribution	Fraction unbound in plasms	BBB	CYP3A4	Clearance	Rat Oral Acute Toxicity	Acute Toxicity Rule
35	2-hexyldecan-1-ol	0.434	0	High	2.429	1.593% L	Excellent	NI/NS	5.515	Low	0
36	Bis(2-methylpropyl) benzene-1,2-dicarboxylate	0.749	0	High	1.326	3.352% L	Excellent	NI/NS	11.028	Low	0
37	Methyl hexadecanoate	0.301	0	High	2.026	1.521% L	Medium	NI/NS	4.995	Low	0
38	7,9-ditert-butyl-1-oxaspiro[4.5]deca-6,9-diene-2,8-dione	0.635	0	High	1.007	15.545% H	Excellent	I/NS	4.681	High	0
39	Tetrapentacontane	0.054	2	Low	8.866	0.12% L	Excellent	NI/NS	3.479	Low	0
40	Dibutyl benzene-1,2-dicarboxylate	0.538	0	High	1.084	3.199% L	Excellent	NI/NS	12.528	Low	0
41	Methyl heptadecanoate	0.271	0	High	2.345	1.462% L	Excellent	NI/NS	4.864	Low	0
42	Tetracontane-1,40-diol	0.069	2	Low	5.367	0.477% L	Excellent	NI/NS	4.873	Low	0
43	Octadecanoic acid	0.271	0	High	2.345	1.462% L	Excellent	NI/NS	4.864	Low	0
44	Methyl 2-hydroxyhexadecanoate	0.374	0	High	1.096	2.735% L	Low	NI/NS	4.939	Low	0
45	Ethyl (9Z,12Z)-octadeca-9,12-dienoate	0.2	1	High	2.809	1.109% L	Medium	I/NS	4.687	Low	0
46	Methyl (E)-octadec-9-enoate	0.204	0	High	3.858	1.015% L	Medium	I/NS	3.469	Low	0
47	Methyl octadecanoate	0.243	0	High	2.647	1.409% L	Excellent	NI/NS	4.767	Low	0
48	Methyl 10-methyloctadecanoate	0.235	1	Low	2.491	1.544% L	Excellent	NI/NS	5.37	Low	0
49	Octacosan-1-ol	0.141	2	Low	4.52	0.936% L	Excellent	NI/NS	4.862	Low	0
50	(Z)-hexadec-7-enal	0.237	0	High	3.735	2.944% L	Poor	NI/NS	3.858	Low	0
51	Pentatriacontane	0.082	2	Low	6.195	0.455% L	Excellent	NI/NS	4.115	Low	0
52	Methyl icosanoate	0.196	2	Low	3.112	1.311% L	Excellent	NI/NS	4.655	Low	0
53	N-[[3,6-dichloro-2,7-bis[2-(diethylamino)ethoxy]fluoren-9-ylidene]amino]-2,2-dimethylpropanamide	0.241	1	High	2.315	1.023% L	Medium	NI/S	6.195	Low	0

I Inhibitor, *S* Substrate, *NI* Non-inhibitor, *NS* Non-substrate, *L* Low, *H* High

Table 3 Binding affinity of test ligands with respective urolithiasis targets by tools pack Autodock Vina

S.no	Target	AutoDock Vina [ΔG (kcal/mol)]					
		L-I	L-II	L-III	L-IV	L-V	L-VI
1	Glutathione-disulfide reductase	-5.6	-6.4	-5.7	-6.2	-5.9	-5.5
2	Glutathione-S-transferase	-5.8	-6.9	-6.2	-5.5	-6.7	-6.2
3	Superoxide dismutase	-5.2	-6.2	-5.6	-5.5	-5.8	-5.6
4	Glutathione peroxidase	-4.6	-5	-5.1	-5.1	-5	-4.8
5	Human calcium-sensing receptor	-6.1	-6.8	-6.4	-6	-6.5	-6.3
6	Matrix metalloproteinase (MMP)-9	-6.1	-6	-6.1	-5.7	-7.5	-6.5
7	MMP2	-6.1	-7.4	-6.2	-5.9	-6.3	-6.8

with Thr125 and Lys131, O1 with Arg148, and O4 with Thr125. O3 forms a weak hydrogen bond with Ser150, whereas C9, C1, and C5 have hydrophobic contact with amino acids Thr125, Lys131, and Arg148, respectively (Fig. 3d). Likewise, C3 and C5 of L-IV form hydrophobic contact with amino acids Lys131 and Arg148. The oxygen atom O2 forms a hydrogen bond with T125 and O4 forms with Ser135, Lys131, Ser135, and Arg148, and C9 forms a weak hydrogen bond with Ser135 (Fig. 3e).

The box coordinates for the target protein 5 were 4×-3×3 Å (center) and 81×89×82 Å (size). The ligand, L-II yielded the highest ΔG for the target protein 5 which was about -6.8 kcal/mol in comparison with other ligands. L-II has shown hydrophobic, hydrogen, and weak hydrogen bonding toward target protein 5. The carbon atoms C13, C14, C12, C10, C14, C3, C13, C4, C3, C1 of L-II forms hydrophobic contact with amino acids Val44, Ala46, Val58, Thr103, Tyr246, Asp178, Gln179, respectively. The oxygen atom O1 is involved in hydrogen bonding with amino acids Ser105 and Lys181 (Fig. 3f).

The box coordinates for the target protein 6 were -1×0×2 Å (center) and 46×36×51 Å (size). The ligand, L-VI yielded the highest ΔG for the target protein 6, which was about -6.5 kcal/mol in comparison with other ligands. L-VI has shown hydrophobic and weak hydrogen bonding toward target protein 6. The carbon atoms, C4, C10, C9, C4, C9, C5 were involved in hydrophobic contact with amino acids Leu222, Val223, Leu243, Tyr248, respectively (Fig. 3g). The box coordinates for the target protein 7 were 8×-3×-2 Å (center) and 85×74×79 Å (size). The L-II yielded the highest ΔG for the target protein (7), which was about -7.4 kcal/mol in comparison with other ligands. L-II has shown hydrophobic and hydrogen bonding towards target protein 7. The carbon atoms, C4, C10, C13, C1, C14 were involved in hydrophobic contact with amino acids Ala479, Gln480, Pro527, Phe572, respectively. Whereas the oxygen atom, O1 was involved in hydrogen bonding with amino acids Gln480, Ile481, and Glu525 (Fig. 3h).

Discussion

In the contemporary era, there have been significant changes in the medical treatment of urolithiasis. Currently, urolithiasis care comprises not only stone removal but also recurrence prevention. ROS, which causes oxidative stress, is one of the key components in the pathogenesis of kidney stone disease. Oxalate causes a rise in the free radical generation that can cause cell death, crystal deposition in the renal tubules, and the development of calcium oxalate stones [33]. As a result, therapy with natural antioxidants may be an appropriate strategy for reducing the oxidative stress and kidney damage brought on by hyperoxaluria. Hence the various extracts of *F. religiosa* seed were evaluated for their antioxidant potency.

In reducing power assay Reductants react with potassium ferricyanide forming potassium ferrocyanide which further reacts with $FeCl_3$ to form an intense Prussian blue complex having maximum absorbance at 700 nm [34]. Reductants' antioxidant effects are dependent on the donation of an atom of hydrogen to break the chain of free radicals. Reductants also interact with certain peroxide precursors, inhibiting the production of peroxide. According to the findings reported, the extracts' notable reducing activity appears to be caused by the presence of polyphenols, which may serve as reductants by giving electrons to free radicals and interacting with them to produce more stable products and put an end to radical chain reactions [35]. The results of our present study revealed that both at the highest concentration and cumulatively *F. religiosa* seed ethyl acetate extract had the highest activity. This might be due to the highest total phenolic content of all extracts as reported in our previous study.

Hydroxyl radicals were generated using ascorbic acid- iron EDTA which were estimated quantitatively. The hydroxyl radical is formed by the oxidation reaction with DMSO to yield formaldehyde, which provides a convenient approach to determine hydroxyl radicals

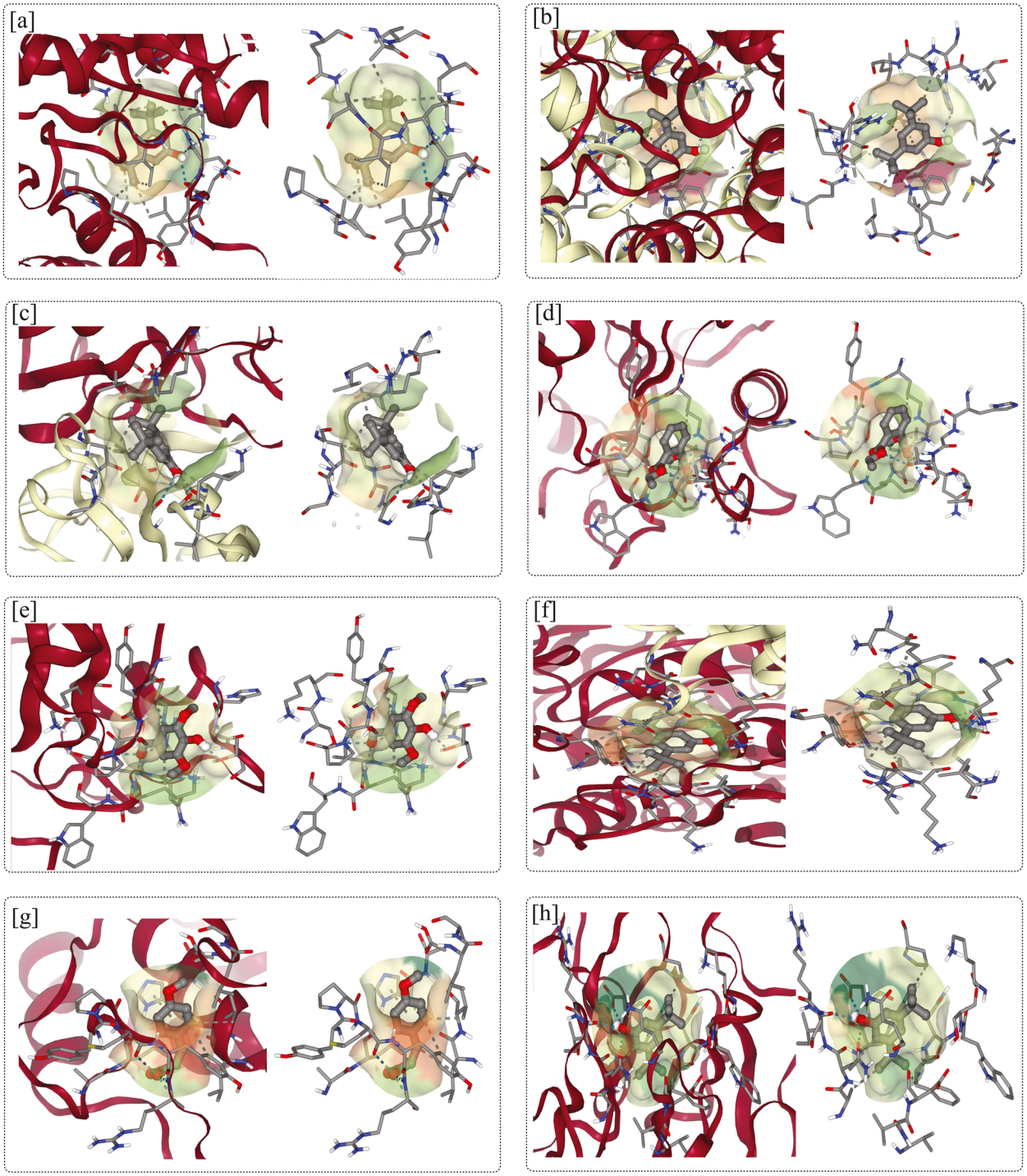

Fig. 3 Binding interactions of **a** Glutathione-disulfide reductase with 3,5-Di-tert-butylphenol, **b** Glutathione-S-transferase with 3,5-Di-tert-butylphenol, **c** Superoxide dismutase with 3,5-Di-tert-butylphenol, **d** Glutathione peroxidase with diethyl benzene-1,2-dicarboxylate, **e** Glutathione peroxidase with 4-hydroxy-3,5-dimethoxybenzaldehyde, **f** Human calcium-sensing receptor with 3,5-Di-tert-butylphenol, **g** Matrix metalloproteinase (MMP)-9 with 2-methoxy-4-prop-2-enylphenol and **h** MMP2 with 3,5-Di-tert-butylphenol by the tools pack Autodock Vina

by treatment with Nash reagent [36]. The extracts' cumulative hydroxyl radical scavenging abilities were discovered to be ethyl acetate > methanol > hexane > chloroform > aqueous in decreasing order. When added to the reaction mixture, each of the *F. religiosa* extracts scavenges hydroxyl radicals in a concentration-dependent manner. The phenolic components in the extracts may have the potential to donate hydrogen, which would explain why the hydroxyl radicals were being scavenged [36].

This test is based on the interaction of GSH with DTNB (also known as Ellman's reagent), which results in the production of the oxidized glutathione-TNB adduct (GS-TNB) and the TNB chromophore, which has a maximum absorbance at 412 nm. The amount of GSH in the sample directly affects how quickly TNB forms which is detected at 412 nm. GSH is subsequently recycled back into the process when GR reduces the disulfide product (GS-TNB) in the presence of NADPH. The quantity of glutathione measured indicates the entire amount of reduced and oxidized glutathione in the sample since GR reduces the GSSG produced into 2GSH([GSH] total = [GSH] + 2 [GSSG]) [37]. The extracts' cumulative hydroxyl radical scavenging abilities were discovered to be ethyl acetate > hexane > chloroform > methanol > aqueous in decreasing order.

The results of GCMS analysis of *F. religiosa* seed extracts gave more precise information about its qualitative phytoconstituents. With the use of GC–MS, volatile non-ionic, thermally stable, and low molecular weight molecules may be found. The flavour and fragrance of any plant are mostly contributed by volatile molecules. The presence of 53 various compounds explains the highest antioxidant activity of ethyl acetate extract when compared to the remaining seed extracts. Although ethyl (9Z,12Z)-octadeca-9,12-dienoate; methyl (E)-octadec-9-enoate; methyl hexadecanoate; octacosan-1-ol are the most abundant components of the extract, these compounds were not that significant in pharmacokinetic aspects. However, some other compounds in the extract showed significant biological activity. 2-Methoxy-4-vinylphenol was reported to be responsible for seed germination inhibition [38], antimicrobial activity [39], anti-inflammatory activity [40]. 3,5-Di-tert-butyl phenol was reported to show antifungal [41], and anti-inflammatory activity [42]. Diethyl benzene-1,2-dicarboxylate was reported to possess antibacterial activity [43]. 4-hydroxy-3,5-dimethoxybenzaldehyde is reported to show antioxidant and antimutagenic activity [44]. 2-methoxy-4-prop-2-enylphenol reportedly has antibacterial activity [45]. bis(2-methyl propyl) benzene-1,2-dicarboxylate in combination with other compounds is reported to show an antimicrobial effect [46].

Drug development is a complicated, perilous, and time-consuming process that can be divided into several stages, including disease-related genomics, target identification/ confirmation, lead discovery/ optimization, and preclinical/ clinical trials [47]. For any compound to act as an effective drug, the molecule must reach its target in the body in ample amounts and stay there long enough in its biologically active form to perform the expected biological event. Drug development involves the assessment of absorption, distribution, metabolism, excretion, and toxicity (ADMET) [48]. Practically, the majority of the time, the final-stage removal of a validated expectant drug is attributed to some unfavourable effectiveness in its ADMET features [49]. In vitro and in vivo ADMET prediction methods have been widely employed recently, although it is impossible to conduct intricate and expensive ADMET experiments on a large number of drugs [25]. Therefore, in silico strategy to predict ADMET properties has become a very attractive, Cost Saving High Throughput alternative to conventional experimental strategies [26]. Lipinski's rule of five states that molecular properties of candidate compounds are required to be within certain ranges for better pharmacokinetics when used through the oral route. The conditions of this rule for compounds are molecular weight < 500, octanol–water partition ratio (LogP) < 5, the total number of hydrogen bond donors ≤ 5, the total number of hydrogen bond acceptors ≤ 10, and molar refractivity between 40–130 [50]. High molecular weight compounds are less likely to cross the membrane bilayer. The compounds whose lipophilicity values are less than 5 are more than 90% likely to have good oral bioavailability [51]. Molar refractivity is related to molecular weight and influences the diffusion coefficient [52]. A high number of hydrogen bond donors and acceptors increases the interaction of the compound with hydrogen-bonding solvents and thereby decreases permeation through the membrane bilayer [51]. In the present study out of the 53 compounds, 38 had zero violations of Lipinski's rule and were fit for oral administration. 9 compounds violated one of the five rules, 3 compounds violated two of the five rules and 3 compounds violated three rules.

As we have contended for the advantages of thinking about drug-likeness in quantitative terms. QED score productively measures and positions targets' druggability as per their related ligands' synthetic appeal. The druggability of targets can be efficiently quantified and ranked using QED [53]. The QED score of the 53 compounds evaluated ranges from 0.141 to 0.749. Compounds having a QED score > 0.67 are considered to be the most suitable drugs. In the present data of 53 compounds, 7 compounds have a QED score > 0.67 which are 2-Methoxy-4-vinyl phenol (0.699), 3,5-Di-tert-butyl

phenol (0.680), diethyl benzene-1,2-dicarboxylate (0.731), 4-hydroxy-3,5-dimethoxybenzaldehyde (0.714), (E)-3-(4-methoxyphenyl)prop-2-enoic acid (0.718), 2-methoxy-4-prop-2-enylphenol (0.693), and bis(2-methyl propyl) benzene-1,2-dicarboxylate (0.749).

Absorption studies give insight into the rate of diffusion of the compound desired to be administered as an oral drug across small intestine or cell monolayers. However, the rate of diffusion is further influenced by several factors like chemical nature, the solubility of the compound as well as P^h of the intestinal secretion, intestinal motility, blood flow, etc. Of all compounds studied for gastrointestinal absorption 69.81% compounds had high absorption.

The study of the volume distribution of a compound assumed to be a potent drug helps us to understand how widely a drug molecule is distributed throughout the body after it is absorbed, as this can determine whether the compound is capable of eliciting a pharmacological response or not [54]. All compounds evaluated in the present study fall in the predicted range (0.04-20L/kg) of VD values according to the ADMETLAB 2.0 tool. Tetrapentacontane has the highest VD value of 8.866 L/Kg and (E)-3-(4-methoxyphenyl)prop-2-enoic acid has the least value of 0.221 L/Kg.

The blood–brain barrier (BBB) prevents drugs from crossing into brain tissue from the blood flow that circulates the body. Drugs used to treat CNS disorders must penetrate the BBB. Lipophilic substances could be able to diffuse across cellular plasma membranes and traverse the BBB in this way. The BBB permeability may be preferentially low or medium for medicines operating on peripheral systems [55]. The compounds evaluated here have different ranges of permeability and hence could be used for central as well as peripheral system treatment.

In pharmacokinetic and pharmacodynamic research, the Fu, *P* value is a significant indicator of drug effectiveness. It is significant as only free drugs, in their unbound state, may move between plasma and tissues and interact with pharmacological target proteins such as receptors, channels, and enzymes. The Fu, P affects renal glomerular filtration and hepatic metabolism, which in turn influences the VD value and total clearance of a drug [56]. Of all compounds evaluated 12 compounds had high Fu, P.

The most significant enzyme system for the metabolism of drugs is cytochrome P450 (CYP), which is made up of a broad family of related isoenzymes [57]. CYP3A4 is the most significant isoenzyme, followed by CYP2D6 and CYP2C9. The main biochemical effect of CYP isoenzymes is to catalyze oxidation, which usually makes the metabolized drug (substrate) more water-soluble and so more readily excreted by the kidneys [58]. Inhibiting CYP3A will boost oral absorption of the drug, reduce hepatic metabolism, and lead to a greater rise in plasma levels [59]. In this study, only 4 compounds are inhibitors of CYP3A4.

When adjusting medication dosages, to achieve a steady state concentration for delivery, clearance value is crucial. Molecules that are excreted out of the body rapidly have higher clearance values. 2-methoxy-4-prop-2-enylphenol shows the highest clearance value of 14.042%.

Forecasting a compound's toxicity is crucial for providing information about potential risks as well as aiding in the identification of the compound's safest dosages. All the compounds of the present study did not show any toxicity in terms of the acute toxicity rule and hence can be considered safe for consumption.

The goal of the current docking investigation was to determine how well certain phytochemicals contained in *F. religiosa* seeds might attach to various protein targets linked to urolithiasis. The phytochemicals were shown to exhibit binding mechanisms with either MMP-2, MMP-9, and human calcium-sensing receptors, as well as a few antioxidant enzymes. The docking results showed variability in the binding affinities as well as in the binding modalities due to the structural diversity among the phytochemicals. Of all the ligands studied ligand II 3,5-Di-tert-butylphenol has shown good binding in terms of binding energies with most of the urolithiasis target proteins (Glutathione-disulfide reductase, Glutathione-S-transferase, Superoxide dismutase, Human calcium-sensing receptor, and MMP2). since 3,5-Di-tert-butylphenol is a phenolic compound this result supports one of the previous studies that reported phenols as potent drugs against renal stones [16].

Likewise, glutathione peroxidase has a good binding with ligand III (diethyl benzene-1,2-dicarboxylate) and ligand IV (4-hydroxy-3,5-dimethoxybenzaldehyde) and MMP-9 with ligand V (2-methoxy-4-prop-2-enylphenol). We cannot infer that ligands have a superior binding efficiency since molecular docking is a static phenomenon but higher binding energy may suggest higher affinity between protein and ligand [60]. Since the grid box was placed across the whole surface of the studied protein, ligands can attach to the protein's many binding locations. However, the study did not show any common amino acid interactions.

Conclusion

The present study revealed that seed extracts of *F. religiosa* had good antioxidant properties comparable to that of standards. The strong antioxidant capacity of these phytochemicals might have strengthened their therapeutic benefits in the treatment of kidney stones and urolithiasis in this case. Based on the bioactive ingredients

present and docking experiments on urolithiasis proteins, this study recommends the use of the *F. religiosa* seed ethyl acetate extract for the treatment of urolithiasis. Experimental research must be carried out to verify each phytochemical's anti-urolithiasis effectiveness in-vitro and in-vivo. These investigations should offer fresh understandings of the fundamental processes through which phytococktails display anti-lithiatic qualities so that they may be used for a variety of lifestyle illnesses improving overall health and well-being.

Abbreviations

ROS	Reactive Oxygen species
MMPs	Matrix metalloproteinases
OPN	Osteogenesis related protein
GST	Glutathione S-transferase
GR	Glutathione disulfide reductase
GPX	Glutathione peroxidase
SOD	Superoxide dismutase
ADMET	Absorption, distribution, metabolism, excretion, toxicity
QED	Quantitative estimate of Druglikeness

Acknowledgements
Authors are thankful to the Central instrumentation laboratory (CIL), Central University of Punjab, Ghudda, Bathinda (CUPB) for providing GC-MS instrumentation.

Authors' contributions
FP is the main contributor to the manuscript, writing, editing, collecting data, and submission/correspondence of the above research article. All authors read and approved the final manuscript.

Funding
Not applicable.

Availability of data and materials
Not applicable.

Declarations

Ethics approval and consent to participate
Not applicable.

Consent for publication
Not applicable.

Competing interests
Not applicable.

Received: 20 July 2023 Accepted: 17 September 2023
Published online: 05 October 2023

References

1. Qian X, Wan J, Xu J, Liu C, Zhong M, Zhang J, et al. Epidemiological trends of urolithiasis at the global, regional, and national levels: a population-based study. Int J Clin Pract. 2022;30(2022):e6807203.
2. Ahmed S, Hasan MM, Mahmood ZA. In vitro urolithiasis models: An evaluation of prophylactic management against kidney stones. J Pharmacogn Phytochem. 2016;5(3):28–35.
3. Evan AP. Physiopathology and etiology of stone formation in the kidney and the urinary tract. Pediatr Nephrol Berl Ger. 2010;25(5):831–41.
4. Khan SR. Reactive oxygen species, inflammation and calcium oxalate nephrolithiasis. Transl Androl Urol. 2014;3(3):256–76.
5. Khan SR. Reactive oxygen species as the molecular modulators of calcium oxalate kidney stone formation: evidence from clinical and experimental investigations. J Urol. 2013;189(3):803–11.
6. Inhibition of autophagy-attenuated calcium oxalate crystal-induced renal tubular epithelial cell injury in vivo and in vitro - PMC [Internet]. Available from:https://www.ncbi.nlm.nih.gov/pmc/articles/PMC5796996/. [Cited 2023 Jun 26].
7. The activation of ROS/NF-κB/MMP-9 pathway promotes calcium-induced kidney crystal deposition - PMC [Internet]. Available from:https://www.ncbi.nlm.nih.gov/pmc/articles/PMC8208877/. [Cited 2023 Jun 26].
8. Narula S, Tandon C, Tandon S. Role of matrix metalloproteinases in degenerative kidney disorders. Curr Med Chem. 2018;25(15):1805–16.
9. Sakamaki Y, Sasamura H, Hayashi K, Ishiguro K, Takaishi H, Okada Y, et al. Absence of gelatinase (MMP-9) or collagenase (MMP-13) attenuates adriamycin-induced albuminuria and glomerulosclerosis. Nephron Exp Nephrol. 2010;115(2):e22-32.
10. Hoesel B, Schmid JA. The complexity of NF-κB signaling in inflammation and cancer. Mol Cancer. 2013;12(1):86.
11. Upregulation of nuclear factor-κB activity mediates CYP24 expression and reactive oxygen species production in indoxyl sulfate-induced chronic kidney disease - PubMed [Internet]. Available from:https://pubmed.ncbi.nlm.nih.gov/26567049/. [Cited 2023 Jun 26].
12. NF–κB activation in renal tubular epithelial cells by oxalate stimulation | Request PDF [Internet]. Available from:https://www.researchgate.net/publication/23188166_NF-kB_activation_in_renal_tubular_epithelial_cells_by_oxalate_stimulation. [Cited 2023 Jun 26].
13. Khan SR, Canales BK. A unified theory on the pathogenesis of Randall's plaques and plugs. Urolithiasis. 2015;43(0 1):109–23.
14. Matrix metalloproteinases, atherosclerosis, proteinuria and kidney disease: linkage–based approaches - PMC [Internet]. Available from:https://www.ncbi.nlm.nih.gov/pmc/articles/PMC4097406/. [Cited 2023 Jun 26].
15. Oxidative Stress in Urolithiasis | IntechOpen [Internet]. Available from:https://www.intechopen.com/chapters/60635. [Cited 2023 Jun 26].
16. Antioxidant and Polyphenol-Rich Ethanolic Extract of Rubia tinctorum L. Prevents urolithiasis in an ethylene glycol experimental model in rats - PMC [Internet]. Available from:https://www.ncbi.nlm.nih.gov/pmc/articles/PMC7917717/. [Cited 2023 Jun 26].
17. Azimi A, Eidi A, Mortazavi P, Rohani AH. Protective effect of apigenin on ethylene glycol-induced urolithiasis via attenuating oxidative stress and inflammatory parameters in adult male Wistar rats. Life Sci. 2021;15(279):119641.
18. Yan F, Yang WK, Li XY, Lin TT, Lun YN, Lin F, et al. A trifunctional enzyme with glutathione S-transferase, glutathione peroxidase and superoxide dismutase activity. Biochim Biophys Acta. 2008;1780(6):869–72.
19. Calcium-sensing receptor and calcium kidney stones - PMC [Internet]. Available from:https://www.ncbi.nlm.nih.gov/pmc/articles/PMC3339356/. [Cited 2023 Jun 26].
20. Xu H, Zisman AL, Coe FL, Worcester EM. Kidney stones: an update on current pharmacological management and future directions. Expert Opin Pharmacother. 2013;14(4):435–47.
21. Agawane SB, Gupta VS, Kulkarni MJ, Bhattacharya AK, Koratkar SS, Rao VK. Patho-physiological evaluation of Duranta erecta for the treatment of urolithiasis. J Ayurveda Integr Med. 2019;10(1):4–11.
22. KVSRG P, D S, K B, K B. Herbal drugs in urolithiasis - a review. Pharmacogn Rev. 2007;1(1):175–9.
23. Sandeep, Kumar A, Dimple, Tomer V, Gat Y, Kumar V. Ficus religiosa: A wholesome medicinal tree. J Pharmacogn Phytochem. 2018;7(4):32–7.
24. Phytochemical Screening of Ficus religiosa Seeds and Evaluation of its Antioxidant Potential. J Food Chem Nanotechnol [Internet]. Available from:https://foodchemistryjournal.com/2022/09/29/phytochemical-screening-of-ficus-religiosa-seeds-and-evaluation-of-its-antioxidant-potential/. [Cited 2023 Jun 26].
25. Patel CN, Kumar SP, Rawal RM, Patel DP, Gonzalez FJ, Pandya HA. A multiparametric organ toxicity predictor for drug discovery. Toxicol Mech Methods. 2020;30(3):159–66.
26. Schyman P, Liu R, Desai V, Wallqvist A. vNN Web Server for ADMET Predictions. Front Pharmacol [Internet]. 2017;8. Available from:https://www.readcube.com/articles/10.3389%2Ffphar.2017.00889. [Cited 2023 Jun 26].

27. Singh S, Gupta P, Gupta J. Virtual structural similarity elucidates bioactivity of fenchone: a phytochemical enriched in fennel essential oil. Curr Drug Discov Technol. 2020;17(5):619–30.
28. Ballabh B, Chaurasia OP, Ahmed Z, Singh SB. Traditional medicinal plants of cold desert Ladakh-used against kidney and urinary disorders. J Ethnopharmacol. 2008;118(2):331–9.
29. Oyaizu, M. Studies on products of browning reactions antioxidative activities of product of browning reaction prepared from glucosamine. Japan J Nutr. 1986;44:307–315. - References - Scientific Research Publishing [Internet]. Available from:https://www.scirp.org/(S(i43dyn45teexjx455qlt3d2q))/reference/ReferencesPapers.aspx?ReferenceID=1125699. [Cited 2023 Jun 26].
30. Klein SM, Cohen G, Cederbaum AI. Production of formaldehyde during metabolism of dimethyl sulfoxide by hydroxyl radical-generating systems. Biochemistry. 1981;20(21):6006–12.
31. Boyne AF, Ellman GL. A methodology for analysis of tissue sulfhydryl components. Anal Biochem. 1972;46(2):639–53.
32. Murail S, Vries SJ de, Rey J, Moroy G, Tuffery P. Seamdock: an interactive and collaborative online docking resource to assist small compound molecular docking. Front Mol Biosci [Internet]. 2021;8. Available from:https://cnrs.hal.science/hal-03677201. [Cited 2023 Jun 26].
33. Herbal medicines in the management of urolithiasis: alternative or complementary? - PMC [Internet]. Available from:https://www.ncbi.nlm.nih.gov/pmc/articles/PMC5693348/. [Cited 2023 Jun 26].
34. Dontha S. A review on antioxidant methods. Asian J Pharm Clin Res. 2016;1:14–32.
35. Loganayaki N, Siddhuraju P, Manian S. Antioxidant activity and free radical scavenging capacity of phenolic extracts from Helicteres isora L. and Ceiba pentandra L. J Food Sci Technol. 2013;50(4):687–95.
36. Pavithra K, Vadivukkarasi S. Evaluation of free radical scavenging activity of various extracts of leaves from Kedrostis foetidissima (Jacq.) Cogn. Food Sci Hum Wellness. 2015;4(1):42–6.
37. Rahman I, Kode A, Biswas SK. Assay for quantitative determination of glutathione and glutathione disulfide levels using enzymatic recycling method. Nat Protoc. 2006;1(6):3159–65.
38. Darabi HR, Mohandessi S, Balavar Y, Aghapoor K. A structure-activity relationship study on a natural germination inhibitor, 2-methoxy-4-vinylphenol (MVP), in wheat seeds to evaluate its mode of action. Z Naturforschung C J Biosci. 2007;62(9–10):694–700.
39. Rubab M, Chelliah R, Saravanakumar K, Barathikannan K, Wei S, Kim JR, et al. Bioactive Potential of 2-Methoxy-4-vinylphenol and Benzofuran from Brassica oleracea L. var. capitate f, rubra (Red Cabbage) on Oxidative and Microbiological Stability of Beef Meat. Foods Basel Switz. 2020;9(5):568.
40. Anti-inflammatory effect of 2-methoxy-4-vinylphenol via the suppression of NF-κB and MAPK activation, and acetylation of histone H3 - PubMed [Internet]. Available from:https://pubmed.ncbi.nlm.nih.gov/22210037/. [Cited 2023 Jun 26].
41. Chen JH, Xiang W, Cao KX, Lu X, Yao SC, Hung D, et al. Characterization of volatile organic compounds emitted from endophytic Burkholderia cenocepacia ETR-B22 by SPME-GC-MS and their inhibitory activity against various plant fungal pathogens. Mol Basel Switz. 2020;25(17):3765.
42. Islam MA, Zilani MNH, Biswas P, Khan DA, Rahman MH, Nahid R, et al. Evaluation of in vitro and in silico anti-inflammatory potential of some selected medicinal plants of Bangladesh against cyclooxygenase-II enzyme. J Ethnopharmacol. 2022;1(285):114900.
43. In vitro antibacterial activity, gas chromatography–mass spectrometry analysis of woodfordia fruticosa kurz. leaf extract and host toxicity testing with in vitro cultured lymphocytes from human umbilical cord blood - sciencedirect [Internet]. Available from:https://www.sciencedirect.com/science/article/pii/S2210909914000873. [Cited 2023 Jun 26].
44. Radioprotection of 4-hydroxy-3,5-dimethoxybenzaldehyde (VND3207) in culture cells is associated with minimizing DNA damage and activating Akt - PubMed [Internet]. Available from:https://pubmed.ncbi.nlm.nih.gov/17981442/. [Cited 2023 Jun 26].
45. Sudarma IM, Darmayanti MG, Sarkono. Antibacterial activities of new and known compounds prepared from eugenol. Rasayan J Chem. 2019;12(02):761–4.
46. Chemical composition and antibacterial properties of achillea micrantha [Internet]. Available from:https://www.ijpsonline.com/articles/chemical-composition-and-antibacterial-properties-of-iachillea-micranthai-3484.html. [Cited 2023 Jun 26].
47. Tang Y, Zhu W, Chen K, Jiang H. New technologies in computer-aided drug design: toward target identification and new chemical entity discovery. Drug Discov Today Technol. 2006;3(3):307–13.
48. Hay M, Thomas DW, Craighead JL, Economides C, Rosenthal J. Clinical development success rates for investigational drugs. Nat Biotechnol. 2014;32(1):40–51.
49. Caldwell GW, Yan Z, Tang W, Dasgupta M, Hasting B. ADME optimization and toxicity assessment in early- and late-phase drug discovery. Curr Top Med Chem. 2009;9(11):965–80.
50. Spriha SE, Rahman SMA. In silico evaluation of selected compounds from Bergenia ciliata (Haw.) Sternb against molecular targets of breast cancer. Indian J Pharm Educ Res. 2022;56(1s):s105-14.
51. Overview on the Rule of Five - PubMed [Internet]. Available from:https://pubmed.ncbi.nlm.nih.gov/22294375/. [Cited 2023 Jun 26].
52. Kuentz MT, Arnold Y. Influence of molecular properties on oral bioavailability of lipophilic drugs - mapping of bulkiness and different measures of polarity. Pharm Dev Technol. 2009;14(3):312–20.
53. Quantifying the chemical beauty of drugs - PMC [Internet]. Available from:https://www.ncbi.nlm.nih.gov/pmc/articles/PMC3524573/. [Cited 2023 Jun 26].
54. Gleeson MP. Generation of a Set of Simple, Interpretable ADMET Rules of Thumb. J Med Chem. 2008;51(4):817–34.
55. Lohmann C, Hüwel S, Galla HJ. Predicting blood-brain barrier permeability of drugs: evaluation of different in vitro assays. J Drug Target. 2002;10(4):263–76.
56. Predicting fraction unbound in human plasma from chemical structure: improved accuracy in the low value ranges | molecular pharmaceutics [Internet]. Available from: https://pubs.acs.org/doi/10.1021/acs.molpharmaceut.8b00785. [Cited 2023 Jun 26].
57. The cytochrome P450 superfamily: biochemistry, evolution and drug metabolism in humans - PubMed [Internet]. Available from:https://pubmed.ncbi.nlm.nih.gov/12369887/. [Cited 2023 Jun 26].
58. Litou C, Effinger A, Kostewicz ES, Box KJ, Fotaki N, Dressman JB. Effects of medicines used to treat gastrointestinal diseases on the pharmacokinetics of coadministered drugs: a PEARRL Review. J Pharm Pharmacol. 2019;71(4):643–73.
59. Wandel C, Kim RB, Kajiji S, Guengerich P, Wilkinson GR, Wood A. P-glycoprotein and cytochrome P-450 3A inhibition: dissociation of inhibitory potencies. Cancer Res. 1999;1(59):3944–8.
60. Patil A, Prakash J, More S, Chandramohan V, Zameer F. Exploring banana phytosterols (Beta-sitosterol) on tight junction protein (claudin) as anti-urolithiasis contributor in Drosophila: a phyto-lithomic approach. Inform Med Unlocked. 2022;1(29):100905.

Publisher's Note

Springer Nature remains neutral with regard to jurisdictional claims in published maps and institutional affiliations.

Submit your manuscript to a SpringerOpen journal and benefit from:

- ► Convenient online submission
- ► Rigorous peer review
- ► Open access: articles freely available online
- ► High visibility within the field
- ► Retaining the copyright to your article

Submit your next manuscript at ► springeropen.com